10-2019

Temporal, spatial, and biological variation of nematode epidemiology in American eels

ZT Warshafsky
Virginia Institute of Marine Science

Troy D. Tuckey
Virginia Institute of Marine Science, tuckey@vims.edu

WK Vogelbein
Virginia Institute of Marine Science, wolf@vims.edu

RJ Latour
Virginia Institute of Marine Science, latour@vims.edu

AR Wargo
Virginia Institute of Marine Science, arwargo@vims.edu

Canadian Science Publishing | Canadian Journal of Fisheries and Aquatic Sciences

TEMPORAL, SPATIAL, AND BIOLOGICAL VARIATION OF NEMATODE EPIDEMIOLOGY IN AMERICAN EELS

Journal:	*Canadian Journal of Fisheries and Aquatic Sciences*
Manuscript ID	cjfas-2018-0136.R2
Manuscript Type:	Article
Date Submitted by the Author:	17-Nov-2018
Complete List of Authors:	Warshafsky, Zoemma; Virginia Institute of Marine Science, Aquatic Health Sciences Tuckey, Troy; Virginia Institute of Marine Science Vogelbein, Wolfgang; Virginia Institute of Marine Science Latour, Robert; Virginia Institute of Marine Science, Fisheries Science Wargo, Andrew; Virginia Institute of Marine Science, Aquatic Health Sciences
Keyword:	EPIDEMIOLOGY < General, PARASITES < Organisms, ESTUARIES < Environment/Habitat, CATADROMOUS SPECIES < Organisms
Is the invited manuscript for consideration in a Special Issue? :	Not applicable (regular submission)

TEMPORAL, SPATIAL, AND BIOLOGICAL VARIATION OF NEMATODE EPIDEMIOLOGY IN AMERICAN EELS

Zoemma T. Warshafsky, Troy D. Tuckey, Wolfgang K. Vogelbein, Robert J. Latour, Andrew R. Wargo. Virginia Institute of Marine Science, College of William & Mary, P.O. Box 1346, Gloucester Point, VA, 23062, USA.

Corresponding author: Z.T. Warshafsky (email: zoemmaw@gmail.com)

ABSTRACT

American eels (*Anguilla rostrata*) are infected by the non-native parasitic nematode *Anguillicoloides crassus*, which can cause severe swimbladder damage. We investigated epidemiology of *A. crassus* to better understand its population-level effects on American eels. Nematode prevalence, abundance, and intensity, and swimbladder damage were quantified in glass eels, elvers, and yellow eels from the lower Chesapeake Bay and related to season of capture, river system, and total length. Age-variant force-of-infection and disease-associated mortality were estimated using a three-state irreversible disease model, which assumes recovery is not possible. Results showed glass eels have very low infection prevalence and severity compared to elvers and yellow eels. Nematode abundance varied by season, river, and eel length, whereas swimbladder damage varied by season and eel length. Nematode abundance and swimbladder damage were weakly positively correlated. Force-of-infection, based on swimbladder damage, peaked at age 2 and disease positive eels had an estimated lower annual survival probability of 0.76 compared to disease negative eels. Full understanding of American eel population dynamics will require broader knowledge of cryptic disease-associated mortality throughout North America.

INTRODUCTION

The American eel (*Anguilla rostrata*) is an economically and ecologically important, yet relatively data-poor, species distributed along the Atlantic coast of North America and throughout the Gulf of Mexico (ASMFC 2012). The American eel population has been declining for the past several decades and is currently considered depleted and at a historically low level of abundance according to the most recent stock assessment update by the Atlantic States Marine Fisheries Commission (ASMFC 2017). Several hypotheses have been proposed to explain the species' decline such as overfishing, pollution, changing climate, altered habitats and food webs, parasites, and emergent disease (Castonguay et al. 1994; Haro et al. 2000). One such proposed hypothesis is the impact of the introduced parasitic nematode, *Anguillicoloides crassus*, which can cause severe damage to the swimbladders of American eels.

Infection by *Anguillicoloides crassus* is endemic in the Japanese eel (*Anguilla japonica*) in Asia, but significant pathology or notable negative population level impacts have not been observed (Sokolowski and Dove 2006). In contrast, the emergence, rapid spread, high prevalence, and pathogenicity of *A. crassus* have been linked to declines in wild European eel (*Anguilla anguilla*) populations and in European eel aquaculture facilities in Asia (Barse et al. 2001; Ooi et al. 1996). Within the American eel population, the parasite was first discovered in 1995 in a Texas aquaculture facility and was first observed in wild animals in South Carolina that same year (Fries et al. 1996). Since its discovery, the distribution of *A. crassus* has expanded rapidly and now occurs in eels in the Gulf of Mexico northward to Nova Scotia (Rockwell et al. 2009). In the Chesapeake Bay, where approximately 60% of the annual U.S. catch of eels is landed (ASMFC 2017), *A. crassus* was first detected in 1997 (Barse and Secor 1999) and

currently can be found in all major tributaries with prevalences as high as 80% (Barse et al. 2001; Fenske et al. 2010).

Eels become infected by consuming intermediate hosts such as copepods and ostrocods or by ingesting paratenic hosts (i.e., intermediate hosts in which parasite development does not occur) such as fishes, amphibians, snails, or insect larvae (Thomas and Ollevier 1992; Moravec 1996; Moravec and Skorikova 1998). Once inside the eel, the parasite moves from the alimentary tract through the body cavity, eventually taking up residence in the swimbladder where it matures, sexually reproduces, and then dies and decays or is forced out through the pneumatic duct (Haenen et al. 1989; De Charleroy et al. 1990). Damage to the eel occurs as a result of larval nematode migration through the swimbladder wall, feeding on blood by adults, and inflammation and degradation of dead adults within the swimbladder lumen (Sokolowski and Dove 2006). Damage clinically manifests as increased opacity, thickening, and pigmentation of the swimbladder wall (Lefevbre et al. 2011). Tissue damage by *A. crassus* can be so severe that it results in complete degradation and loss of swimbladder function (Molnar et al. 1995; Wurtz et al. 1996; Kobyashi et al. 1990). However, the adverse health impacts of this infection and its impacts on eel population dynamics are not well understood, in part due to a complex relationship between parasite abundance and degree of swimbladder damage, suggesting that severe damage may prevent subsequent infections (Lefevbre et al. 2013).

Previous studies addressing the impacts of *A. crassus* have mainly focused on infection prevalence and mean intensity (Fenske et al. 2010; Aieta and Oliveria 2009; Hein et al. 2014), but these metrics may provide an inaccurate or incomplete characterization of the multifaceted epidemiology. Potential discrepancies in the relationship between parasite abundance and swimbladder damage may be caused by intermediate and paratentic host dynamics, *A. crassus*

dying within the swimbladder and decaying or being cleared, and the possibility that a highly damaged swimbladder may not serve as a suitable habitat for *A. crassus* (De Charleroy et al. 1990; van Banning and Haenen 1990). Additionally, previous analyses have focused mainly on yellow eels and have not included younger life stages, despite potential susceptibility of those stages to infection (Hein et al. 2015; De Charelory et al. 1990). Finally, it is not known if *A. crassus* causes infection-associated mortality (Lefebvre et al. 2013), which greatly limits understanding of the population level impacts of this parasite in American eels.

The objectives of our study were to (1) quantify prevalence, abundance, and intensity of *Anguillicoloides crassus* infections in glass, elver, and yellow stage American eels in the Chesapeake Bay; (2) clarify the relationships between parasite abundance and swimbladder damage and the impacts of capture location, eel size, and season on the infection; and (3) model *A. crassus* force of infection in Chesapeake Bay, including exploration of spatiotemporal covariate effects, and evaluate disease-associated morality. Collectively, our results support ongoing American eel management efforts by addressing key questions related to patterns in disease prevalence and population impacts of *A. crassus*.

METHODS

Field collections

Glass and elver stage American eels were collected from six sites within the lower Chesapeake Bay from March through June 2015 using Irish eel ramps (Figure 1). Traps were placed in areas of freshwater runoff and a dam that impeded the eels' upstream movements. The six sites were on the James River (Wareham's Pond), York River (Bracken's Pond and Wormley

Pond), Rappahannock River (Kamp's Millpond), and Potomac River (Clark's Millpond and Gardy's Millpond). Sampling was conducted according to protocols established by the ASMFC for monitoring young-of-year glass eels (ASMFC 2012). Traps were checked a minimum of two days per week, with increasing frequency depending on the strength of glass eel ingress. On the first sampling day of each week, a maximum of 30 glass eels and 20 elvers were collected if possible, followed by up to 10 glass eels and 5 elvers each subsequent sampling day depending on their availability. This sampling technique was designed to optimize collecting enough eels to detect the nematode at low prevalence and reducing potential sampling biases such as autocorrelation within a catch (i.e., pseudoreplication associated with cluster sampling). Differentiation between glass eels and elvers was based on pigmentation stage (Haro and Kruger 1988), with fully pigmented eels considered elvers, and the incompletely pigmented eels considered glass eels.

Yellow stage American eels were collected from 2013 to 2015 by the VIMS Seine Survey and Juvenile Fish Trawl Survey (Tuckey and Fabrizio 2013) and opportunistically from the Virginia Department of Game and Inland Fisheries Electrofishing Survey. The Trawl and Seine Surveys sampled eels in primarily brackish and tidal fresh water, whereas the Electrofishing Survey sampled eels in mainly freshwater locations. Yellow eels were collected within the James, York, and Rappahannock River watersheds from all three surveys, whereas yellow eels in the Potomac River watershed were collected exclusively by electrofishing.

Laboratory processing

Weights (nearest 0.001 g) and lengths (nearest 0.01 mm total length) were obtained from glass eels and elvers that were euthanized using clove oil, measured, and then frozen (-18°C) for

storage. Yellow eels were euthanized using an ice slurry, frozen immediately, and weighed (nearest 0.1 g) and measured (nearest 1 mm) following thawing just prior to dissection. For all eels, the swimbladder was removed after thawing and opened to enumerate adult *A. crassus*. Counts of larval *A. crassus* in the swimbladder wall were quantified for glass eels under a dissecting microscope, after placing the swimbladder between two glass slides. Only adult *A. crassus* parasites were recorded for elvers and yellow eels. Swimbladder condition was quantified using the Swimbladder Degenerative Index (SDI; Lefevbre et al. 2002). This index quantifies three swimbladder attributes—bladder wall opacity, thickness, and pigmentation and exudate (e.g. dead worms, erythrocytes, decaying swimbladder tissue, eggs, and L2 stage of *A. crassus*; Lefebvre et al. 2002) with each of these ranked from 0 (healthy, normal condition) to 2 (severe condition). The three attribute scores were added together to generate a total SDI ranging from 0 to 6. Due to the difficulty of detecting eggs and L2 stage *A. crassus* in swimbladders, these two types of exudate were not used to determine the presence of exudate in elvers and yellow eels, but were used in glass eel analyses.

Sagittal otoliths were extracted from elvers and yellow eels and processed for age determination (Michaud et al. 1988; Cieri and McCleave 2000; Morrison and Secor 2003). Otoliths were mounted on a glass slide with CrystalBond™ and sanded down in the frontal plane until the core was visible. The otolith was then flipped and the opposite end was sanded down until the otolith was transparent and annuli were clearly visible. Annuli were quantified using a compound microscope. Each otolith was read independently by two readers and those specimens with annulus counts that differed were read again. Final age assignments were based on consensus between readers. Because eels have been in the Atlantic Ocean for about one year prior to metamorphosing into glass eels and the first annulus may not be laid down until after a

full year in coastal waters (ASMFC 2017), one year was added to all ages. Protocols for sampling and euthanizing eels were approved by the College of William & Mary's Institutional Animal Care and Use Committee.

Statistical analyses

Infection prevalence (proportion of eels infected with nematodes), mean abundance (average number of nematodes across all eels surveyed, infected and uninfected), and mean infection intensity (average number of nematodes per infected eel) were calculated from all eel stages and river systems using adult *A. crassus* counts (Bush et al. 1997). Glass eel analysis included both the adult and larval stages of the parasite. For all following analyses, a plausible set of candidate model parameterizations was defined based on hypotheses regarding potential effects of covariates (i.e., the covariates included in models have been shown to be important in other studies or represent plausible hypotheses unique to this study). Final models were selected using a combination of goodness of fit measures and Akaike's Information Criterion value (AIC; Burnham and Anderson 2002).

Parasite abundance

For glass eels, the probability of infection by *A. crassus* larval and adult stages combined in relation to glass eel total length (TL) was investigated using a binomial generalized linear model with a logit link function. The inflection point, or the TL at which the probability of being infected is 0.5, of the binomial model was calculated and its standard error was estimated using the delta-method (Seber 1982). Glass eels were excluded from subsequent analyses due to low prevalence and infection intensity.

For elvers and yellow eels, preliminary analyses comparing AIC values of the fully statured model (all covariates in both count and zero model components) to the fully saturated count model that includes only the intercept in the zero component indicated that parasite count data were zero-inflated (i.e., an excess frequency of zeros in the dataset; ΔAIC = 74.6). Therefore zero-inflated negative binomial models were used to explore the effects of covariates on parasite abundance and the probability of a false zero, or the absence of parasites due to design, survey, or observation error (Zuur et al. 2012). The covariates included river system (James, York, Rappahannock, Potomac), season (created by assigning the date of capture into the four seasons based on the solstices and equinoxes of that year), SDI, and TL. Multiple model parameterizations were considered that reflected different combinations of covariates for the count and false zero model components. The dispersion parameter ($d = \sum \frac{residual^2}{df(residual)}$), which indicates overdispersion when $d > 1$, and the Pearson residual versus fitted value plots were used to evaluate goodness of fit of the models. Partial predictions from the most empirically supported model were generated using marginal means (Searle et al. 1980).

SDI

The swim bladder degenerative index (SDI) is an ordered categorical response variable, requiring a specific regression framework to capture the sequential nature of the data. The ordinal logistic regression (or cumulative logit model) meets this requirement by modelling the probability of an eel having a certain level of swimbladder damage (i.e., SDI score) or lower against all higher levels (Agresti 2010; Hedeker 2003; McCullagh 1980) such that:

$$logit(P(Y_{ij} \leq c)) = \theta_c - (\boldsymbol{x}_{ij}^t \boldsymbol{\beta} + \boldsymbol{u}_{ij}^t \boldsymbol{\alpha}_c + v_i) \quad (1)$$

The cumulative $logit(P(Y_{ij} \leq c))$ represents the cumulative probability of the j^{th} eel from the i^{th} catch having a c^{th} level of swimbladder damage. The parameter θ_c represents strictly increasing model thresholds $(1, ..., C-1)$. The covariate vector $\boldsymbol{x}_{ij}$, which includes the intercept, follows the proportional odds assumption such that there is only one vector of regression parameters $\boldsymbol{\beta}$ for each covariate. Covariate vector $\boldsymbol{u}_{ij}$ follows partial proportional odds such that there is a different vector of regression parameters $\boldsymbol{\alpha}_c$ for every level of c for each covariate (Agresti 2010; Hedeker 2003; McCullagh 1980). The parameter v_i is the random effect for catch i distributed $N(0,\sigma_v^2)$. Odds ratios $(Y \geq j)$ are obtained through exp $(\boldsymbol{\beta})$, and indicate the odds ratio of a swimbladder having a damage level c or higher for a given level of a covariate (Agresti 2010; Hedeker 2003; McCullagh 1980).

The proportional odds assumption (or parallel regression assumption), states that the odds ratios of the different levels of a covariate are equal across all thresholds of swimbladder damage levels, necessitating only one $\boldsymbol{\beta}$ coefficient. For example, for a given covariate (e.g. season), the ratio of the odds of having a certain swimbladder damage level in one season (e.g. spring) to the odds of having the same swimbladder condition in another season (e.g. winter) are equal across all thresholds of swimbladder damage levels. This does not mean that the odds of swimbladder damage within one level of a covariate are equal, but instead that the odds ratios of two levels of a covariate are equal (i.e. proportional odds). This assumption can be relaxed by utilizing partial proportional odds, which allows coefficient $\boldsymbol{\alpha}_c$ to vary with thresholds of SDI scores and therefore not have equal odds ratios between levels of a covariate.

This approach was used to explore the effects of covariates river system, TL, season, parasite abundance, and catch ID (random effect) on the odds of having attained greater than or equal to the c^{th} level of swimbladder damage. Due to low sample size of higher parasite

intensities, a plus group was defined such that intensities ranged from zero to 10+. To aid convergence and model interpretation, SDI scores were condensed into three ordered levels (low: 0-1, moderate: 2-3, severe: 4-6, such that $c = 0, 1, 2$). The proportional odds assumption was evaluated by fitting multiple models with and without covariates as partial proportional odds, and AIC was used for model selection. Overall goodness of fit was evaluated using the condition number of the Hessian, for which values larger than 10^6 indicate that the model may be ill defined (Christensen 2015). Partial predictions from the model with the most empirical support were generated using marginal means (Searle et al. 1980).

Epidemiology

To estimate the probability that an uninfected eel becomes infected, termed force-of-infection (FOI), and evaluate the potential presence of infection-associated mortality, we applied a three-state irreversible disease model (see Heisey et al. 2006 for full details). The model is designed to provide estimates of key epidemiological parameters from cross-sectional (i.e. data representing multiples ages or cohorts) from binary prevalence-at-age data (i.e. either disease positive or disease negative at a given age). The model assumes no vertical transmission (i.e., transmission from mother to offspring) or recovery to a state of full health. Force-of-infection can be either age-invariant or age-dependent, and the Weibull, Pareto, Gompertz, and log-logistic hazard functions were evaluated to identify the appropriate functional shape of the FOI curve (Heisey et al. 2006). The model also allows for estimation of an additive disease-associated mortality parameter that represents the additional mortality rate experienced by disease-positive individuals relative to the background mortality rate of disease-negative individuals.

The effects of covariates month, season, and river system (all categorical) on force-of-infection were investigated using log-linear models such that:

$$\lambda(t) = \lambda_0(t)e^{X\beta}. \quad (2)$$

The age-dependent FOI, denoted $\lambda(t)$, is modeled as the baseline FOI, λ_0 adjusted by the effects of covariates included in the design matrix *X* and the associated vector of parameters β (Heisey et al. 2006). The covariate month was redefined to represent two-month time periods (six levels) starting with January/February. Due to low sample size of older eels, a plus group was defined so that ages ranged from 1 to 12+. Disease-positive eels were those that had a swimbladder with an SDI score ≥ 3. Because *A. crassus* can die within the swimbladder and degrade or be expelled through the pneumatic duct, prevalence does not meet the no-recovery assumption of the force of infection model (i.e., damage to the swimbladder has occurred, but an absence of parasites does not accurately capture the damage). As such, force-of-infection modelling was not conducted on infection prevalence data.

All statistical analyses were performed using the R software package (R Core Team 2014). The 'pscl' package was used for fitting zero-inflated GLMs (Zeileis et al. 2008) and the 'ordinal' package (Christensen 2015) was used for fitting ordinal logistic regression models. Results are presented as the mean or estimate ± standard error.

RESULTS

Anguillicoloides crassus infection and disease in glass eels

A total of 1480 glass eels were collected from all six sites ranging in total length from 47.3 to 77.5 mm (mean: 57.6 mm ± 0.103). Adult and larval nematode counts in glass eels were

combined and yielded an overall infection prevalence of 3.2%, mean nematode abundance per eel of 0.047 ± 0.009 (range: 0-10), and mean infection intensity of 1.46 ± 0.195. Only glass eels collected in the Potomac and Rappahannock rivers were infected (Table 1). Glass eels had higher infection levels of the larval stage of *A. crassus* (prevalence: 2.5%, mean abundance: 0.039 ± 0.009, mean intensity: 1.57 ± 0.25, range: 0-10) compared to the adult stage (prevalence: 0.8%, mean abundance: 0.008 ± 0.002, mean intensity: 1 ± 0, range: 0-1). The probability of infection by larval and adult nematodes combined increased with the length of glass eels (Figure 2). The TL with a 0.5 probability of being infected was 78.3 ± 2.8 mm. Furthermore, only the more advanced pigment stages of glass eels were found to be infected with larval and adult *A. crassus*, and only the highest pigment stages of 5 and 6 showed any swimbladder damage. Overall, minimal swimbladder damage was found with only seven glass eels having scores greater than 0 (mean SDI: 1.14 ± 0.143).

A. crassus infection and disease in elver and yellow eels

Across all six sampling sites, a total of 814 elvers were collected and total length ranged from 49.0 to 238.0 mm (mean: 113.8 mm ± 1.02). Adult nematode prevalence was 59.2%, mean abundance per eel was 1.51 ± 0.061, mean intensity per infected eel was 2.44 ± 0.072, and average SDI was 1.62 ± 0.055. When summarized by river system, James River elvers showed the highest prevalence (66.7%), average abundance (1.83 ± 0.13), mean intensity (2.73 ± 0.13), and average SDI (1.82 ± 0.11); however the difference in mean infection and disease levels between sites was small (Table 1). There was substantial variation between individual elvers such that infection intensity ranged from 0 to 10 nematodes and the full range of SDI scores (0-6) was observed.

A total of 973 yellow eels were collected across all four river systems and all three surveys. Total length of these individuals ranged from 60.0 to 700.0 mm (mean: 285.9 mm ± 3.71). Adult nematode prevalence was 46.2%, mean abundance per eel was 1.35 ± 0.079, mean intensity per infected eel was 2.92 ± 0.136, and average SDI was 2.44 ± 0.055. Yellow eels from the Potomac River showed the highest prevalence (55.2%), whereas those from the Rappahannock River exhibited the highest mean abundance (1.53 ± 0.13) and mean intensity (3.09 ± 0.22). Those from the James River displayed the highest average SDI (2.3 ± 0.08), although mean differences between sites was again small (Table 1). As with elvers, there was substantial variation among individuals in infection intensity and disease, such that infection intensity in yellow eels ranged from 0 to 28 nematodes and the full range of SDI scores (0-6) was observed.

Parasite abundance

The full zero-inflated negative binomial with river system, season, TL, and SDI as covariates for both the zero-inflated and count components of the model received the most empirical support (i.e., lowest AIC score; Table S1), had a dispersion parameter value close to one (1.16), and the Pearson residual versus fitted value plot showed this model fit the data well. This model was closely followed (ΔAIC <2, dispersion = 1.15) by a model without SDI in the zero-inflated component. Due to the importance of SDI in the analysis and the lower AIC, the full model was selected for inference.

When comparing parasite abundance (Table 2) using the count model, the estimated effect for the Potomac River indicated lower mean parasite abundance relative to the James River (-0.452 ± 0.112), whereas the estimated effects of the Rappahannock and York Rivers also

314 indicated lower mean parasite, though much smaller in magnitude (-0.135 ± 0.103 and -0.015 ±
315 0.103 respectively, Figure 3). Regarding season, the estimated effects of spring and summer
316 indicated similar higher mean parasite abundances relative to fall (0.294 ± 0.130 and 0.224 ±
317 0.138 respectively), whereas winter showed a lower mean parasite abundance (-0.149 ± 0.316,
318 Figure 3). The estimated effect of TL indicated a positive relationship to parasite abundance
319 ($1.37x10^{-3} \pm 4.42x10^{-4}$). However, due to zero-inflation, the relationship between TL and
320 predicted parasite count was dome-shaped; the exception being both the Potomac River across
321 all seasons and winter across all river systems where the relationship was continuously
322 increasing due to very low zero-inflation (Figure 3). For SDI, parasite abundance was higher for
323 all scores compared to the baseline (SDI 1: 0.279 ± 0.124, SDI 2: 0.512 ±0.116, SDI 3: 0.295 ±
324 0.131, SDI 4: 0.502 ± 0.156, SDI 5: 0.387 ± 0.194, SDI 6: 0.500 ± 0.238, Figure 3).
325
326 **Swimbladder condition**
327 The ordinal logistic regression model with the most empirical support included TL as a
328 proportional odds covariate, season and parasite abundance as partial proportional odds
329 covariates, and catch ID as a random effect (Tables 3 and S2). Inclusion of the random factor
330 resulted in a significant drop in AIC (ΔAIC = 128.7), despite only a few eel catches appearing to
331 drive the effect (Figure S1), and therefore it was selected for inference. The condition number of
332 the Hessian for the selected model was 1.3×10^7, which is slightly above the recommended value
333 of 10^6. Dropping season from the model resulted in a lower Hessian value of 6.5×10^6, but raised
334 the AIC (ΔAIC = 8). The results for the other covariates were unchanged between the two
335 models, so season was ultimately included in the final model.

This model indicated that increasing TL was associated with an increase in the odds of having a more damaged swimbladder (0.004 ± 0.001, Figure 4). As such, the longer an eel, the more likely it has a more damaged swimbladder. Also, the overall trend between parasite abundance and swimbladder damage was a positive relationship. The parasite abundance coefficients were negative (low versus moderate/severe condition: -0.2 ± 0.04 and low/moderate versus severe condition: -0.12 ± 0.04) yet, when added to the positive model intercepts (low versus moderate/severe condition: 0.39 ± 0.29 and low/moderate versus severe condition: 3.15 ± 0.31), the sum of the log odds was still a positive value. Therefore, increasing parasite abundance resulted in an increased probability of swimbladder damage, but this increased probability was reduced by the underlying negative relationship (Figure 4). The effect of season was minimal, with only the estimated effect of having a severely damaged swimbladder in the summer relative to fall indicating a decreased odds (-0.8 ± 0.29, Figure 4).. The odds among the three swimbladder conditions were not found to differ between the other seasons and fall (i.e. estimates ± standard error overlapped zero, Figure 4). Overall, eels had a higher predicted probability of having a moderately damaged swimbladder (0.566 ± 0.063) compared to a low (0.310 ± 0.042) or severely (0.124 ± 0.051) damaged swimbladder.

Force of infection and disease associated mortality

Sixty-four elvers and 661 yellow eels were included in the force of infection analysis, ranging in age from 1 to 16 years (age range of 1 to 12+ used in analysis due to small sample size of older individuals). Observed prevalence of swimbladder damage increased steeply from age 1 to 2 and then slowed to a slight increase with age, whereas observed prevalence of *A.*

358 *crassus* infection was highest in the younger and older eels but lower in the middle ages (Figure
359 5).

360 Age-dependent force-of-infection models received more support than age-invariant
361 models when fitted to prevalence of swimbladder damage data (Table 4). The model with the
362 most empirical support was the log-logistic with month pairs and the mortality term, though
363 several other models were within three AIC units (Table 4). Across hazard models parameterized
364 with the same set of covariates, inclusion of the mortality term lowered the AIC for all except for
365 the Gompertz models (Table 4). Additionally, the combination of month pairs and the morality
366 term resulted in the lowest AIC value within each set of hazard models, excluding the Gompertz
367 hazard models (Table 4). The unit hazard ratios (i.e., proportional difference in force of
368 infection) for month pairs relative to the baseline of November/December were
369 January/February: 0.026, March/April: -0.793, May/June: -0.294, July/August: -0.430, and
370 September/October: -0.486. Force of infection peaked at age 2 and then decreased with
371 subsequent ages (Figure 6). The disease-associated mortality term was estimated as 0.277 (95%
372 CI: 0.0845-0.507) and the annual survival ratio of a diseased eel relative to a non-diseased eel is
373 $e^{-(-0.277)}$ (Heisey et al. 2006) or 0.76 (95% CI: 0.602-0.919).

374 Other cutoffs of swimbladder damage level considered indicative of infection (i.e. SDI $\geq$
375 1, 2, 4, 5, or 6) were explored. Similar results were found in these analyses such that the
376 mortality term was included in either the model with the most empirical support or in models
377 within 2 AIC units of the selected model. Additionally, month was usually (4 out of 6 cases) a
378 covariate in the model with the most empirical support. Likewise, force of infection peaked at
379 age 2 in almost all cases (Figure S3).
380

DISCUSSION

Our study indicates that *A. crassus* infection and resultant swimbladder pathology vary across host developmental stages and are influenced by environmental factors experienced by American eels, which may ultimately result in disease-associated mortality. Infection prevalences of over 50% were found in elvers and yellow eels, compared to only 2.5% in glass eels. In general, similar patterns were observed in several previous studies of *A. crassus* in the Chesapeake Bay region (Barse and Secor 1999; Barse et al. 2001; Fenske et al. 2010). Low infection prevalence in glass eels, also observed by Hein et al. (2015) in South Carolina, are potentially due to less time in the estuary and therefore less exposure to *A. crassus*, given that eels first come in contact with the parasite in coastal waters (Van Banning and Haenen 1990). This conclusion is also supported by finding mostly larval stage nematodes in glass eels in our study, although Hein et al. (2015) found only adult nematodes. This difference could be due to sampling location—glass eels in our study were caught in more brackish downstream sites (with the exception of our Potomac sites) where they were most likely first exposed to *A. crassus*, and eels collected in the South Carolina study were caught further up-river allowing more time for infection by larval *A. crassus* and develop into adults (Hein et al. 2015). Our analyses also indicated that season, size, and age differences in susceptibility, transmission, and mortality could be drivers of observed in variation of infection and disease for elver and yellow eels.

Season appeared to be a minor source of variation in parasite abundance and swimbladder damage for elver and yellow eels in our study. Parasite abundance was higher in spring and lower during winter, whereas severe swimbladder damage had the highest probability in summer and lowest in winter, though this effect was weak. These seasonal dynamics may be

driven by eel behavior and the abundance of *A. crassus* in the environment. For example, eels are believed to be dormant in the cooler winter months (Kennedy and Fitch 1990), but as the water warms in spring, they become active and commence feeding, which likely increases their exposure to *A. crassus* through consumption of intermediate and paratenic hosts. Additionally, at lower temperatures, the reproductive cycle of the parasite slows (Kim et al. 1989; Nagasawa et al. 1994; Knopf et al. 1998), which may reduce parasite abundance and swimbladder damage in the colder months. Seasonal differences could therefore indicate the existence of a lag between acquiring parasites in the spring and accumulating damage from these parasites in the summer, although future research is needed to explore the timing of infection and how this relates to swimbladder damage.

For both parasite abundance and swimbladder damage, TL had a positive relationship. By including zero-inflation in our analysis of parasite abundance, we were able to reveal that the highest parasite abundances occur around 300 mm TL relatively consistently across seasons, river systems, and swimbladder conditions. The mechanisms behind this relationship are unknown, but it is likely that as eels get larger, they consume more prey and are more exposed to *A. crassus*. Larger eels also have bigger swimbladders, which may provide more habitat for the parasite. It is then possible that after eels reach a certain size, various aspects of parasite and swimbladder damage accumulation drive prevalence downwards, possibly through disease associated mortality as shown in the force of infection model. Evidence of such confounding effects was supported by our finding that swimbladder damage was positively correlated with eel length, but weakly correlated with parasite abundance.

River system was also found to be a potential source of variation in parasite abundance, but not swimbladder damage. In particular, the Potomac River had overall lower parasite

abundance compared to the other river systems. These variations in infection, transmission, and disease by season, size, and site observed in our study could be explained by a variety of environmental and ecological factors (Hein et al. 2014; Moser et al. 2001; Fenske et al. 2010; Hein et al. 2015; Morrison and Secor 2003; Machut and Limburg 2008; Aieta and Oliveira 2009). For example, higher salinity has been shown to have a negative effect on *A. crassus* infection (Kirk et al. 2000; Lefebvre and Crivelli 2012), but we could not investigate this covariate because we did not measure salinity in this study. Additionally, different locations and seasons could have different availabilities of *A. crassus* or intermediate hosts and could vary with other factors such as temperature, which could impact *A. crassus* transmission and infection levels in eels (De Charleroy et al. 1989; Kennedy and Fitch 1990; Molnar et al. 1991; Molnar 1993). These and other environmental parameters warrant further investigation.

Parasite abundance and swimbladder damage are two metrics useful in characterizing *A. crassus* infection, although we found that they are weakly correlated; a higher parasite abundance may not directly correlate to more swimbladder damage. Although the estimated mean parasite abundance was highest for the highest SDI score of 6 and lowest for the lowest SDI score of 0, intermediate values of the metrics did not increase directly linearly. Additionally, at higher parasite abundances, the probabilities of having a severely damaged swimbladder versus a mildly damaged swimbladder were almost indistinguishable. Yet moderate damage had an overall higher probability across the range of parasite abundances. A nonlinear relationship was also found by several studies on European eels (Lefebvre et al. 2002; Lefebvre et al. 2013), but is not well documented for American eels.

The nonlinear relationship between parasite count and swimbladder damage may be caused by various aspects of the complex relationship between *A. crassus* and American eels.

Nematodes can die within the swimbladder and degrade or be cleared out, but leave behind damaged tissue. Also, there may be a lag between nematode presence and damage accumulation such that multiple infections may occur before damage accrues (Van Banning and Haenen 1990; Molnar et al 1993; Wurtz and Tarachewski 2000). Additionally, density dependence among *A. crassus* exists such that more adult nematodes within the lumen can arrest further movement of larval nematodes into the lumen (Ashworth and Kennedy 1999). Furthermore, as a swimbladder becomes more damaged, it becomes a less suitable habitat for nematodes (Van Banning and Haenen 1990; Molnar et al. 1993). Therefore, a swimbladder can be in poor condition but it may have no nematodes within it or it can appear healthy and harbor many parasites. Lefevbre et al. (2002, 2013) suggested that the health state of the swimbladder may be a better long-term indicator of overall infection history than number of living nematodes present at a given time. Nematode count represents parasite pressure at a single point in time, whereas swimbladder damage shows past and present damage, thereby potentially giving a more comprehensive indication of infection severity.

The complexities in the dynamics of disease also likely play a role in the transmission, or force of infection, of the parasite. The peak of FOI at age-2 indicated that most eels first become infected shortly after entering the estuary. However, it is important to note that in this study FOI was modeled using swimbladder damage rather than prevalence of the nematode, and how long it takes infection to result in detectable disease is unknown. If, as our previous analyses indicate, there is a lag between infection and swimbladder damage, our FOI results could also suggest that eels acquire the majority of nematodes in the spring, which then results in peak visible swimbladder damage in the summer months. This is consistent with our findings that parasite abundance is highest in the spring and severe swimbladder damage is highest in the summer.

Eels likely do not accumulate more damage in the spring because they are not becoming re-infected in the winter due to dormancy and lack of feeding (Kennedy and Fitch 1990) as indicated by the lower FOI in March/April.

Importantly, the FOI model indicated that there is lower annual survival of eels with moderate to severe swimbladder damage compared to those with very low or no damage. This finding is supported by the overall low probability of eels having a severely damaged swimbladder; if severe damage increases the likelihood of mortality, then there would a lower chance of catching eels with such badly damaged swimbladders. Previous studies have shown that higher *A. crassus* infection prevalence and intensity affect the ability of eels to swim, tolerate hypoxic conditions or high temperatures, avoid hydraulic dams, and avoid predators and fishing pressure (Molnar et al. 1991; Molnar 1993; Gollock et al. 2005; Lefebvre and Crivelli 2007), creating potential sources of elevated mortality. Because the FOI model is not able to differentiate between mortality and recovery, more research is needed to determine if recovery could also be occurring. The ability of the swimbladder to recover from infection is speculated but not definitely shown to occur (Molnàr et al. 1994; Szèkely et al. 2005; Lefebvre et al. 2012). It is possible that due to the widespread availability of *A. crassus* intermediate and paratenic hosts and the lack of acquired immunity (Knopf 2006), eels may be constantly exposed to the nematode and never have the opportunity or ability to fully recover, although partial healing of the swimbladder could be possible. Clearance of individual nematodes from the swimbladder through either decay or forced exit through the pneumatic duct would result in fewer nematodes within the swimbladder and would represent recovery by the definition of the FOI model if disease prevalence is defined as nematode prevalence. Yet, the relationship between parasite load and swimbladder damage is complex and fewer parasites does not necessarily mean a less

damaged organ. For these reasons, *A. crassus* infection prevalence was determined to not be a suitable parameter for the FOI model.

In conclusion, parasite load and swimbladder damage, although related, illustrate different components of this complex host parasite relationship. Parasite abundance shows parasite pressure at a given point in time, whereas swimbladder damage is integrative and likely represents the accumulation of disease and its negative impacts over time. Additionally, we have shown that *A. crassus* infection may contribute to American eel mortality and therefore may require consideration in future American eel stock assessments. A better understanding of the timeline of the lifecycle of *A. crassus* would make it possible to determine if fluctuations in parasite abundance and swimbladder damage are due to parasite availability or mortality. These fluctuations could also be better informed with information regarding the lag between nematode infection and swimbladder damage, in addition to the ability for eels to recover from infection.

ACKNOWLEDGEMENTS

This work was funded by the Virginia Sea Grant Graduate Research Fellowship and a Virginia Institute of Marine Science Foundation Fellowship. The research would not have been possible without the generous help from the VIMS young-of-year American Eel survey, which collected glass eels and elvers and was funded by the Virginia Marine Resources Commission (VMRC; through the Recreational Fishing Advisory Board and the Commercial Fishing Advisory Board), as well as the Potomac River Fisheries Commission. Additionally, the VIMS Juvenile Fish Trawl Survey and Striped Bass Seine Survey (funded by VMRC and Federal Aid to Sport Fish Restoration and the Commonwealth of Virginia) collected yellow eels for this study. The map in Figure 1 was created by Debra Gauthier of the Multispecies Research Group at VIMS. We would like to thank two anonymous reviewers for valuable feedback. We also appreciate the generous cooperation of the Virginia Department of Game and Inland Fisheries, in particular Aaron Bunch, who organized the collection of yellow eels from various electrofishing

surveys around the state and allowed us to use their data for this research. This paper is Contribution No. 3791 of the Virginia Institute of Marine Science, College of William & Mary.

REFERENCES

Agresti, A. 2010. Analysis of ordinal categorical data. John Wiley & Sons, Hoboken, NJ.

Aieta, A.E., and Oliveira, K. 2009. Distribution, prevalence, and intensity of the swimbladder parasite *Anguillicola crassus* in New England and eastern Canada. Dis. Aquat. Organ. 84: 229–35. doi:10.3354/dao02049.

Ashworth, S.T., and Kennedy, C.R. 1999. Density-dependent effects on *Anguillicola crassus* (Nematoda) within its European eel definitive host. Parasitology 118(3): 289–296.

Atlantic States Marine Fisheries Commission. 2012. American Eel Benchmark Stock Assessment for Peer Review. Stock Assessment Report No. 12-01.

Barse, A.M., Mcguire, S.A., Vinores, M.A., Eierman, L.E., and Weeder, J.A. 2001. The swimbladder nematode *Anguillicola crassus* in American eels (*Anguilla rostrata*) from middle and upper regions of Chesapeake Bay. J. Parasitol. 87(6): 1366–1370. doi:10.1645/0022-3395(2001)087[1366:TSNACI]2.0.CO;2.

Barse, A.M., and Secor, D.H. 1999. An exotic nematode parasite of the American eel. Fisheries 24(2): 6–10. doi:10.1577/1548-8446(1999)024.

Bush, A.O., Lafferty, K.D., Lotz, J.M., and Shostak, A.W. 1997. Parasitology meets ecology on its own terms: Margolis et al. revisited. J. Parasitol. 83(4): 575–583. doi:10.2307/3284227.

Burnham, K.P., and Anderson, D.R. 2002. Model selection and inference: a practical information-theoretic approach, Springer, New York, NY.

Castonguay, M., Hodson, P.V., Couillard, C.M., Eckersley, M.J., Dutil, J.-D., and Verreault, G. 1994. Why is recruitment of the American eel, *Anguilla rostrata*, declining in the St. Lawrence River and Gulf? Can. J. Fish. Aquat. Sci. 51(2): 479–488. doi:10.1139/f94-050.

Christensen, R.H.B. 2015. A tutorial on fitting cumulative link models with the ordinal package [online]. Available from https://cran.r-project.org/web/packages/ordinal/vignettes/clm_tutorial.pdf [accessed 14 August 2017].

Cieri, M.D., and McCleave, J.D. 2000. Discrepancies between otoliths of larvae and juveniles of the American eel: is something fishy happening at metamorphosis? J. Fish Biol. 57: 1189–1198. doi:10.1006/jfbi.2000.1381.

De Charleroy, D., Grisez, L., Thomas, K., Belpaire, C., and Ollevier, F. 1990. The life cycle of *Anguillicola crassus*. Dis. Aquat. Organ. 8: 77–84. doi:10.3354/dao008077.

De Charleroy, D., Thomas, K., Belpaire, C., and Ollevier, F. 1989. The viability of the free living larvae of *Anguillicola crassus*. J. Appl. Ichthyol. 5: 154–156. doi:10.1111/j.1439-0426.1989.tb00487.x.

Fenske, K.H., Secor, D.H., and Wilberg, M.J. 2010. Demographics and parasitism of American eels in the Chesapeake Bay, USA. Trans. Am. Fish. Soc. 139(6): 1699–1710. doi:10.1577/T09-206.1.

Fries, L.T., Williams, D.J., and Johnson, S.K. 1996. Notes: Occurrence of *Anguillicola crassus*, an exotic parasitic swim bladder nematode of eels, in the southeastern United States. Trans. Am. Fish. Soc. 125(5): 794–797. doi:10.1577/1548-8659(1996)125<0794:NOOCAE>2.3.CO;2.

Gollock, M.J., Kennedy, C.R., and Brown, J.A. 2005. European eels, *Anguilla anguilla* (L.), infected with *Anguillicola crassus* exhibit a more pronounced stress response to severe hypoxia than uninfected eels. J. Fish Dis. 28: 429–436. doi:10.1111/j.1365-2761.2005.00649.x.

Haenen, O.L.M., Grisez, L., De Charleroy, D., Belpaire, C., and Ollevier, F. 1989. Experimentally induced infections of European eel *Anguilla anguilla* with *Anguillicola crassus* (Nematoda, Dracunculoidea) and subsequent migration of larvae. Dis. Aquat. Organ. 7: 97–101. doi:10.3354/dao007097.

Haro, A., Richkus, W., Whalen, K., Hoar, A., Busch, W.-D., Lary, S., Brush, T., and Dixon, D. 2000. Population decline of the American eel: implications for research and management. Fisheries 25(9): 7–16. Taylor & Francis Group. doi:10.1577/1548-8446(2000)025<0007:PDOTAE>2.0.CO;2.

Haro, A.J., and Krueger, W.H. 1988. Pigmentation, size, and migration of elvers (Anguilla rostrata (Lesueur)) in a coastal Rhode Island stream. Can. J. Zool. 66: 2528–2533. doi:10.1139/z88-375.

Hedeker, D. 2003. A mixed-effects multinomial logistic regression model. Stat. Med. 22: 1433–1446. https://doi.org/10.1002/sim.1522

Hein, J.L., Arnott, S.A., Roumillat, W.A., Allen, D.M., and de Buron, I. 2014. Invasive swimbladder parasite *Anguillicoloides crassus*: infection status 15 years after discovery in wild populations of American eel *Anguilla rostrata*. Dis. Aquat. Organ. 107: 199–209. doi:10.3354/dao02686.

Hein, J.L., Buron, I. De, Roumillat, W.A., Post, W.C., Hazel, A.P., and Arnott, S.A. 2015. Infection of newly recruited American eels (*Anguilla rostrata*) by the invasive swimbladder parasite *Anguillicoloides crassus* in a US Atlantic tidal creek. ICES J. Mar. Sci.: 1–8. doi:10.1093/icesjms/fsv097.

Heisey, D.M., Joly, D.O., and Messier, F. 2006. The fitting of general force-of-infection models to wildlife disease prevalence data. Ecology 87(9): 2356–2365. doi:10.1890/0012-9658(2006)87[2356:TFOGFM]2.0.CO;2.

Kennedy, C.R., and Fitch, D.J. 1990. Colonization, larval survival and epidemiology of the nematode *Anguillicola crassus*, parasitic in the eel, *Anguilla anguilla*, in Britain. J. Fish Biol. 36: 117–131. doi:10.1111/j.1095-8649.1990.tb05588.x.

Kim, Y.-G., Kim, E.-B., Kim, J.-Y., and Chun, S.-K. 1989. Studies on a nematode, *Anguillicola crassus* parasitic in the air bladder of the eel. J. fish Pathol. 2(1): 1–18.

Kirk, R.S., Kennedy, C.R., and Lewis, J.W. 2000. Effect of salinity on hatching, survival and infectivity of *Anguillicola crassus* (Nematoda: Dracunculoidea) larvae. Dis. Aquat. Organ. 40: 211–218. doi:10.3354/dao040211.

Knopf, K. 2006. The swimbladder nematode *Anguillicola crassus* in the European eel *Anguilla anguilla* and the Japanese eel *Anguilla japonica*: differences in susceptibility and immunity between a recently colonized host and the original host. J. Helminthol. 80: 129–136. doi:10.1079/JOH2006353.

Knopf, K., Naser, K., van der Heijden, M.H., and Taraschewski, H. 2000. Humoral immune response of European eel *Anguilla anguilla* experimentally infected with *Anguillicola crassus*. Dis. Aquat. Organ. 42(1): 61–9. doi:10.3354/dao042061.

Knopf, K., Würtz, J., Sures, B., and Taraschewski, H. 1998. Impact of low water temperature on the development of *Anguillicola crassus* in the final host *Anguilla anguilla*. Dis. Aquat. Organ. 33: 143–149. doi:10.3354/dao033143.

Kobayashi, H., Pelster, B., and Scheid, P. 1990. CO2 back-diffusion in the rete aids O2 secretion in the swimbladder of the eel. Respir. Physiol. 79(3): 231–242. doi:10.1016/0034-5687(90)90129-M.

Lefebvre, F., Contournet, P., and Crivelli, A.J. 2002. The health state of the eel swimbladder as a measure of parasite pressure by *Anguillicola crassus*. Parasitology 124: 457–463. doi:10.1017/S0031182001001378.

Lefebvre, F., Contournet, P., and Crivelli, A.J. 2007. Interaction between the severity of the infection by the nematode *Anguillicola crassus* and the tolerance to hypoxia in the European eel *Anguilla anguilla*. Acta Parasitol. 52(2): 171–175. doi:10.2478/s11686-007-0013-4.

Lefebvre, F., and Crivelli, A.J. 2012. Salinity effects on Anguillicolosis in Atlantic eels: A natural tool for disease control. Mar. Ecol. Prog. Ser. 471: 193–202. doi:10.3354/meps10032.

Lefebvre, F., Fazio, G., Mounaix, B., and Crivelli, A.J. 2013. Is the continental life of the European eel *Anguilla anguilla* affected by the parasitic invader *Anguillicoloides crassus*? Proc. R. Soc. B 280: 20122916. doi:10.1098/rspb.2012.2916.

Lefebvre, F., Fazio, G., Palstra, A.P., Székely, C., and Crivelli, A.J. 2011. An evaluation of indices of gross pathology associated with the nematode *Anguillicoloides crassus* in eels. J. Fish Dis. 34: 31–45. doi:10.1111/j.1365-2761.2010.01207.x.

Machut, L.S., and Limburg, K.E. 2008. *Anguillicola crassus* infection in *Anguilla rostrata* from small tributaries of the Hudson River watershed, New York, USA. Dis. Aquat. Organ. 79: 37–45. doi:10.3354/dao01901.

McCullagh, P. 1980. Regression Models for Ordinal Data. J. R. Stat. Soc. **B.** 42: 109–142.

Michaud, M., Dutil, J.-D., and Dodson, J.J. 1988. Determination of the age of young American eels, in fresh water, based on otolith surface area and microstructure. J. Fish Biol. 32: 179–189. doi:10.1111/j.1095-8649.1988.tb05351.x.

Molnár, K. 1993. Effects of decreased oxygen content on eels (*Anguilla anguilla*) infected by *Anguillicola crassus* (Nematoda: Dracunculoidae). Acta Vet. Hunganca 43(3–4): 349–360.

Molnár, K., Baska, F., Csaba, G., Glavits, R., and Szekely, C. 1993. Pathological and histopathological studies of the swimbladder of eels *Anguilla anguilla* infected by *Anguillicola crassus* (Nematoda: Dracunculoidea). Dis. Aquat. Organ. 15: 41–50. doi:10.3354/dao015041.

Molnár, K., Szakolczai, J., and Vetési, F. 1995. Histological changes in the swimbladder wall of eels due to abnormal location of adult and second stage larvae of *Anguillicola crassus*. Acta Vet. Hung. 43(1): 125–137.

Molnár, K., Székely, C., and Baska, F. 1991. Mass mortality of eel in Lake Balaton due to *Anguillicola crassus* infection. Bull. Eur. Assoc. Fish Pathol. 11(6): 211–212.

Molnár, K., Székely, C., and Perényi, M. 1994. Dynamics of *Anguillicola crassus* (Nematoda: Dracunculoidea) infection in eels of Lake Balaton, Hungary. Folia Parasitol. (Praha). 41: 193–202. doi:10.1017/CBO9781107415324.004.

Moravec, F. 1996. Aquatic invertebrates (snails) as new paratenic hosts of *Anguillicola crassus* (Nematoda: Dracunculoidea) and the role of paratenic hosts in the life cycle of this parasite. Dis. Aquat. Org. 27: 237–239. doi:10.3354/dao027237.

Moravec, F., and Skoríková, B. 1998. Amphibians and larvae of aquatic insects as new paratenic hosts of *Anguillicola crassus* (Nematoda: Dracunculoidea), a swimbladder parasite of eels. 34(1996): 217–222. doi:10.3354/dao034217.

748 Morrison, W.E., and Secor, D.H. 2003. Demographic attributes of yellow-phase American eels
749 (*Anguilla rostrata*) in the Hudson River estuary. Can. J. Fish. Aquat. Sci. 60: 1487–1501.
750 doi:10.1139/f03-129.
751
752 Moser, M.L., Patrick, W.S., and Jr., J.U.C. 2001. Infection of American eels, *Anguilla rostrata*,
753 by an introduced nematode parasite, *Anguillicola crassus*, in North Carolina. Available
754 from http://www.asihcopeiaonline.org/doi/abs/10.1643/0045-
755 8511(2001)001%5B0848:IOAEAR%5D2.0.CO%3B2 [accessed 22 September 2014].
756
757 Nagasawa, K., Kim, Y.-G., and Hirose, H. 1994. *Anguillicola crassus* and *A. globiceps*
758 (Nematoda: Dracunculoidea) parasitic in the swimbladder of eels (*Anguilla japonica* and
759 *A. anguilla*) in East Asia: A review. Folia Parasitol. (Praha). 41: 127–137.
760
761 Ooi, H.K., Wang, W.S., Chang, H.Y., Wu, C.H., Lin, C.C., and Hsieh, M.T. 1996. An epizootic
762 of Anguillicolosis in cultured American eels in Taiwan. J. Aquat. Anim. Health 8(2):
763 163–166. doi:10.1577/1548-8667(1996)008<0163:AEOAIC>2.3.CO;2.
764
765 R Core Team. 2017. R: A language and environment for statistical computing. R Foundation for
766 Statistical Computing, Vienna, Austria. URL https://www.R-project.org/.
767
768 Rockwell, L.S., Jones, K.M.M., and Cone, D.K. 2009. First Record of *Anguillicoloides crassus*
769 (Nematoda) in American Eels (*Anguilla rostrata*) in Canadian Estuaries, Cape Breton,
770 Nova Scotia. J. Parasitol. 95(2): 483–486. doi:10.1645/GE-1739.1.
771
772 Seber. 1982. The Estimation of Animal Abundance, 2nd ed. Griffin, London.
773
774 Searle, S.R., Speed, F.M., and Milliken, G.A. 1980. Population marginal means in the linear
775 model: an alternative to least squares means. Am. Stat. 34(4): 216–221.
776 doi:10.1080/00031305.1980.10483031.
777
778 Sokolowski, M.S., and Dove, A.D.M. 2006. Histopathological examination of wild American
779 eels infected with *Anguillicola crassus*. J. Aquat. Anim. Health 18(4): 257–262.
780 doi:10.1577/H06-009.1.
781
782 Székely, C., Molnár, K., and Rácz, O.Z. 2005. Radiodiagnostic method for studying the
783 dynamics of *Anguillicola crassus* (Nematoda: Dracunculoidea) infection and pathological
784 status of the swimbladder in Lake Balaton eels. Dis. Aquat. Organ. 64: 53–61.
785 doi:10.3354/dao064053.
786
787 Thomas, K., and Ollevier, F. 1992. Population biology of *Anguillicola crassus* in the final host
788 *Anguilla anguilla*. Dis. Aquat. Organ. 14: 163–170.
789
790 Tuckey, T.D., and Fabrizio, M.C. 2013. Influence of survey design on fish assemblages:
791 implications from a study in Chesapeake Bay Tributaries. Trans. Am. Fish. Soc. 142(4):
792 957–973. doi:10.1080/00028487.2013.788555.
793

Van Banning, P. and Haenen, O.L.M. 1990. Effects of the swimbladder nematode *Anguillicola crassus* in wild and farmed eel, *Anguilla anguilla*. *In* Pathology in marine science. *Edited by* F.O. Perkins and T.C. Cheng. Academic Press, New York, NY. pp. 317−330.

Wang, C.H., and Tzeng, W.N. 1998. Interpretation of geographic variation in size of American eel *Anguilla rostrata* elvers on the Atlantic coast of North America using their life history and otolith ageing. Mar. Ecol. Prog. Ser. 168: 35–43. doi:10.3354/meps168035.

Würtz, J., and Taraschewski, H. 2000. Histopathological changes in the swimbladder wall of the European eel *Anguilla anguilla* due to infections with *Anguillicola crassus*. Dis. Aquat. Organ. 39: 121–134. doi:10.3354/dao039121.

Würtz, J., Taraschewski, H., and Pelster, B. 1996. Changes in gas composition in the swimbladder of the European eel (*Anguilla anguilla*) infected with *Anguillicola crassus* (Nematoda). Parasitology 112: 233–238. doi:10.1017/S003118200008481X.

Zeileis, A., Kleiber, C., and Jackman S. 2008. Regression models for count data in R. Journal of Statistical Software. **27**:8.

Zuur, A.F., Saveliev, A.A., and Ieno, E.N. 2012. Zero Inflated Models and Generalized Linear Mixed Models. Highland Statistics Limited.

840 **TABLES**
841
842 Table 1. Prevalence (%), mean abundance (SE; range), and mean intensity (SE) of
843 *Anguillicoloides crassus,* and swimbladder degenerative index (SDI; SE) in American eels by
844 river system and eel stage.
845

Location	Stage	N	Prevalence (%)	Abundance	Intensity	SDI
Potomac	Glass	116	5.2	0.05 (0.02; 0-1)	1 (0)	0.02 (0.01)
	Elver	269	59.6	1.26 (0.09; 0-10)	2.11 (0.11)	1.81 (0.1)
	Yellow	29	55.2	1.21 (0.24; 0-4)	2.19 (0.23)	1.97 (0.38)
	Total	414	44	0.91 (0.07; 0-10)	2.08 (0.1)	1.28 (0.08)
Rappahannock	Glass	249	2.4	0.02 (0.01; 0-1)	1 (0)	0.01 (0.01)
	Elver	114	53.3	1.13 (0.15; 0-9)	2.13 (0.2)	1.1 (0.17)
	Yellow	379	49.7	1.53 (0.13; 0-21)	3.09 (0.22)	1.03 (0.15)
	Total	742	34.2	0.96 (0.08; 0-21)	2.82 (0.17)	1.43 (0.06)
York	Glass	744	0	0 (0)	0 (0)	0.002 (0.002)
	Elver	230	64.8	1.72 (0.13; 0-10)	2.66 (0.15)	1.52 (0.1)
	Yellow	153	45.1	1.23 (0.23; 0-28)	2.77 (0.45)	2.85 (0.15)
	Total	1127	18.6	0.5 (0.05; 0-28)	2.7 (0.18)	0.67 (0.04)
James	Glass	371	0	0 (0)	0 (0)	0.01 (0.003)
	Elver	201	66.7	1.83 (0.13; 0-7)	2.73 (0.13)	1.82 (0.11)
	Yellow	412	43	1.24 (0.11; 0-18)	2.88 (0.19)	2.3 (0.08)
	Total	984	50.6	1.43 (0.08; 0-18)	2.82 (0.12)	1.32 (0.05)

Table 2. Model components and estimates from the most empirically supported model describing the effects of covariates on count of *Anguillicoloides crassus* in American eels.

Model Component	Parameter	Level	Estimate	Standard Error
Zero-inflated	River system	James	Baseline	N/A
		Potomac	-16.8	0.002
		Rappahannock	-0.423	0.295
		York	-0.357	0.288
	Season			
		Fall	Baseline	N/A
		Winter	-12.5	225
		Spring	0.724	0.358
		Summer	0.746	0.375
	Total length		0.0064	0.001
	SDI			
		0	Baseline	N/A
		1	-1.36	0.470
		2	-0.656	0.620
		3	-0.758	0.359
		4	-1.19	0.503
		5	-0.402	0.464
		6	-1.48	1.11
Count (negative binomial)	River system			
		James	Baseline	N/A
		Potomac	-0.452	0.112
		Rappahannock	-0.135	0.103
		York	-0.015	0.103
	Season			
		Fall	Baseline	N/A
		Winter	-0.149	0.316
		Spring	0.294	0.130
		Summer	0.224	0.138
	Total length		0.0014	4×10^{-4}
	SDI	0	Baseline	N/A
		1	0.279	0.124
		2	0.512	0.116
		3	0.295	0.131
		4	0.502	0.156
		5	0.387	0.194
		6	0.500	0.238

Table 3. Model components and estimates from the most empirically supported model describing the effects of covariates on swimbladder damage (low = 0, moderate = 1, severe = 2) from *Anguillicoloides crassus* in American eels. The "|" symbol in SDI Threshold indicates the threshold between swimbladder damage levels of the swimbladder degenerative index (SDI) for which the estimate of partial proportional odds applies for a given parameter. For example, 0|1 indicates the probability an eel has an SDI of 0 versus all higher scores. Random effect estimate is the variance ± standard deviation.

Parameter type	**Parameter**	**SDI Threshold**	**Estimate**	**Standard Error**
Intercepts		0|1	0.387	0.288
		1|2	3.15	0.310
Proportional odds	Total Length		0.0042	0.001
Partial proportional odds	Season	0|1 fall	Baseline	N/A
		1|2 fall	Baseline	N/A
		0|1 winter	-0.425	0.911
		1|2 winter	0.641	0.971
		0|1 spring	0.204	0.251
		1|2 spring	-0.049	0.267
		0|1 summer	0.091	0.282
		1|2 summer	-0.800	0.294
	Parasite count	0|1	-0.201	0.036
		1|2	-0.117	0.036
Random effect	Catch ID		1.423	1.197

Table 4. Assessment of force-of-infection model fits for presence of swimbladder damage (SDI ≥ 2) in American eels based on Akaike's information criterion. Months were grouped in to pairs starting with January/February (i.e. month pairs). Catch sites were grouped by river system (Potomac, Rappahannock, York, James Rivers). μ is the disease associated mortality term.

	ΔAIC					
Infection hazard model	Null	μ	Season	Season, μ	System	System, μ
constant	40.6	7	35.1	11	40.3	6.5
Weibull	13.8	9	18.6	12.8	12	8.4
Pareto	9.2	7.5	13.9	11.8	8.5	7.9
Gompertz	5.3	7	10.4	11.6	5.5	7.5
log-logistic	11.2	3	15.7	6.4	10.4	5.5

	ΔAIC					
Infection hazard model	Season, System	Season, System, μ	Month pairs	Month pairs, μ	Month pairs, System	Month pairs, System, μ
constant	35.1	10.8	27.8	3.4	31.8	6.3
Weibull	17	12.5	10.2	5.3	11.9	8.2
Pareto	13.4	12.4	6.1	4.7	8.5	7.9
Gompertz	12.5	10.7	3.1	4.7	5.9	7.9
log-logistic	15.2	9.4	6.3	0	9.3	4.8

898
899 **FIGURES**

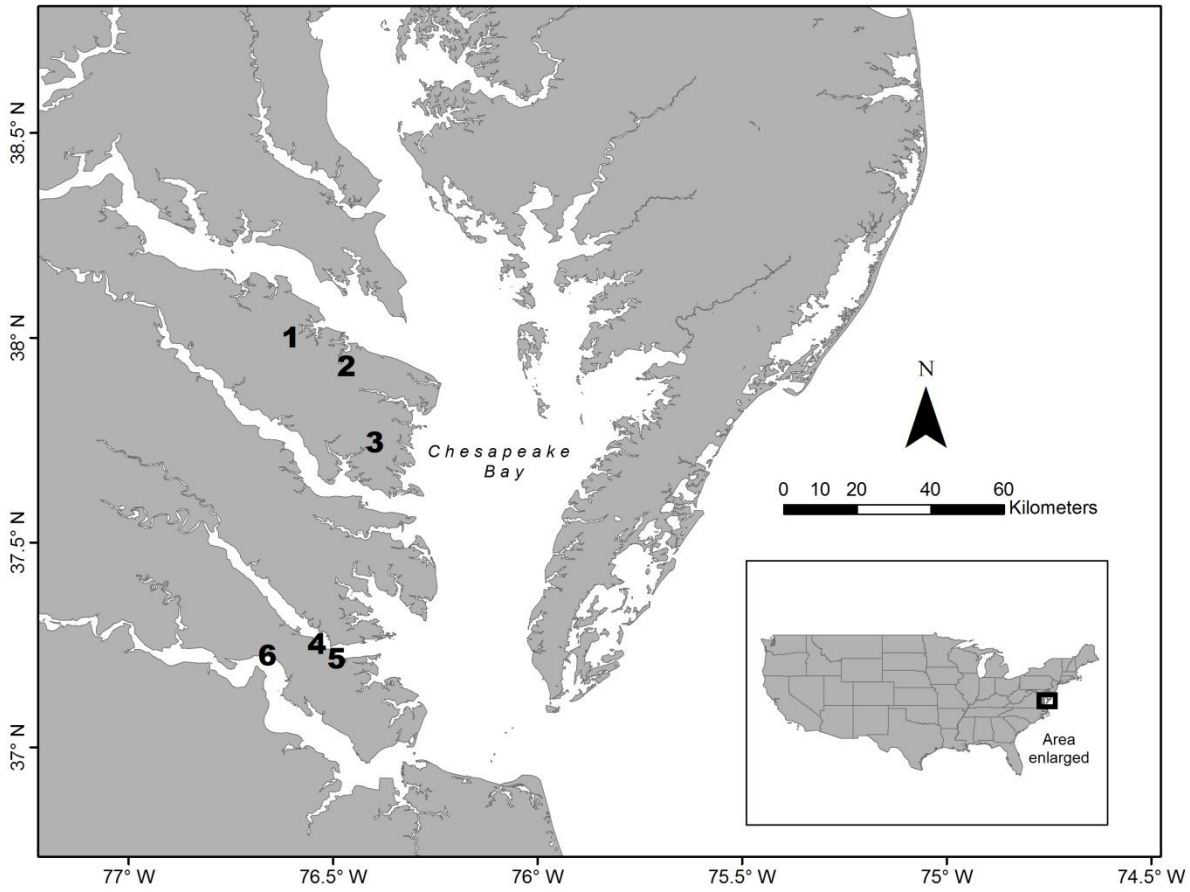

900
901
902 Figure 1. Map of collection sites for glass and elver American eels from lower Chesapeake Bay,
903 USA. Potomac River: (1) Gardy's Millpond, (2) Clark's Millpond; Rappahannock River: (3)
904 Kamp's Millpond; York River: (4) Bracken's Pond, (5) Wormley Pond; James River: (6)
905 Wareham's Pond. Map data from Arcinfo produced by Environmental Systems Research
906 Institute (ESRI, 1987).
907
908

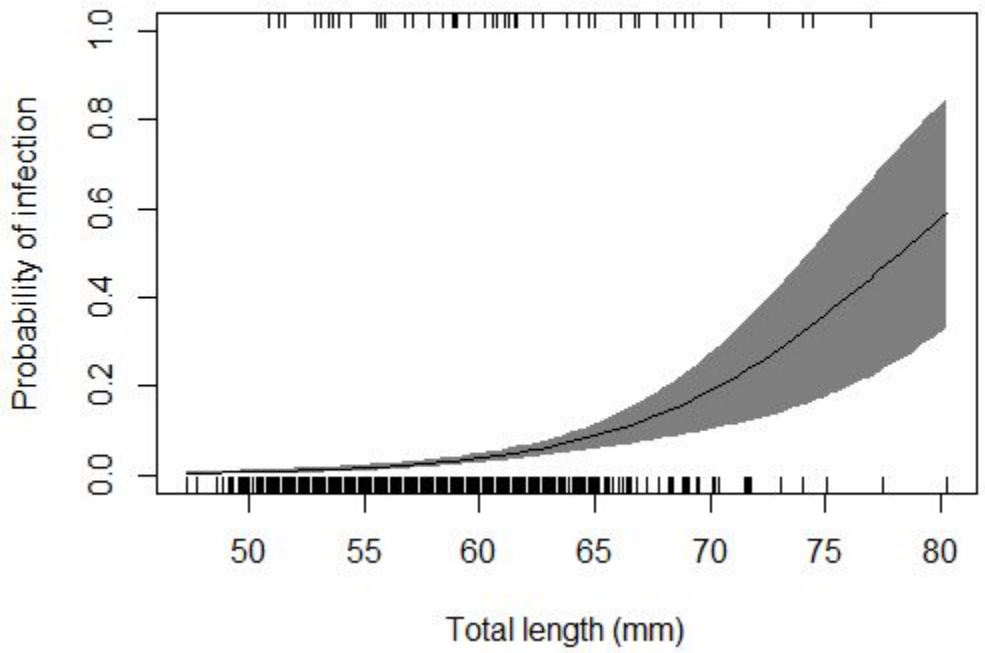

Figure 2. Probability of infection with larval and adult *Anguillicoloides crassus* by total length (mm) for glass eels. Black line represents binomial model results with 95% CI (grey shaded area). Tick marks are individual eel observations of infected (top of plot) or uninfected (bottom of plot).

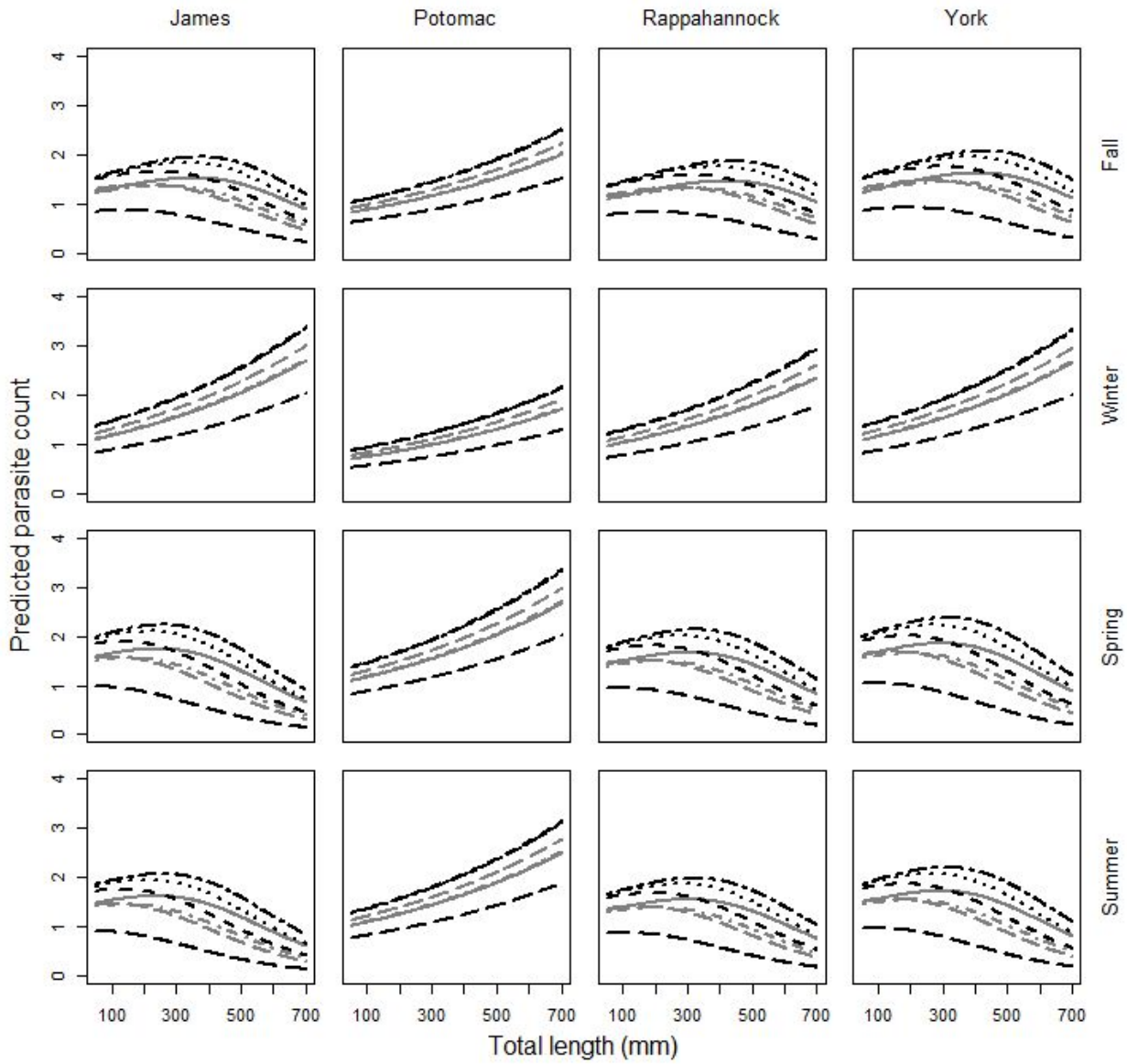

Figure 3. Predicted *Anguillicoloides crassus* parasite count for elver and yellow American eels for season of capture, system, total length (mm), and swimbladder degenerative index (SDI) total score. Results are from a zero-inflated negative binomial model. Individual lines represent SDI scores: 0 = , 1 = , 2 = , 3 = , 4 = , 5 = , 6 = .

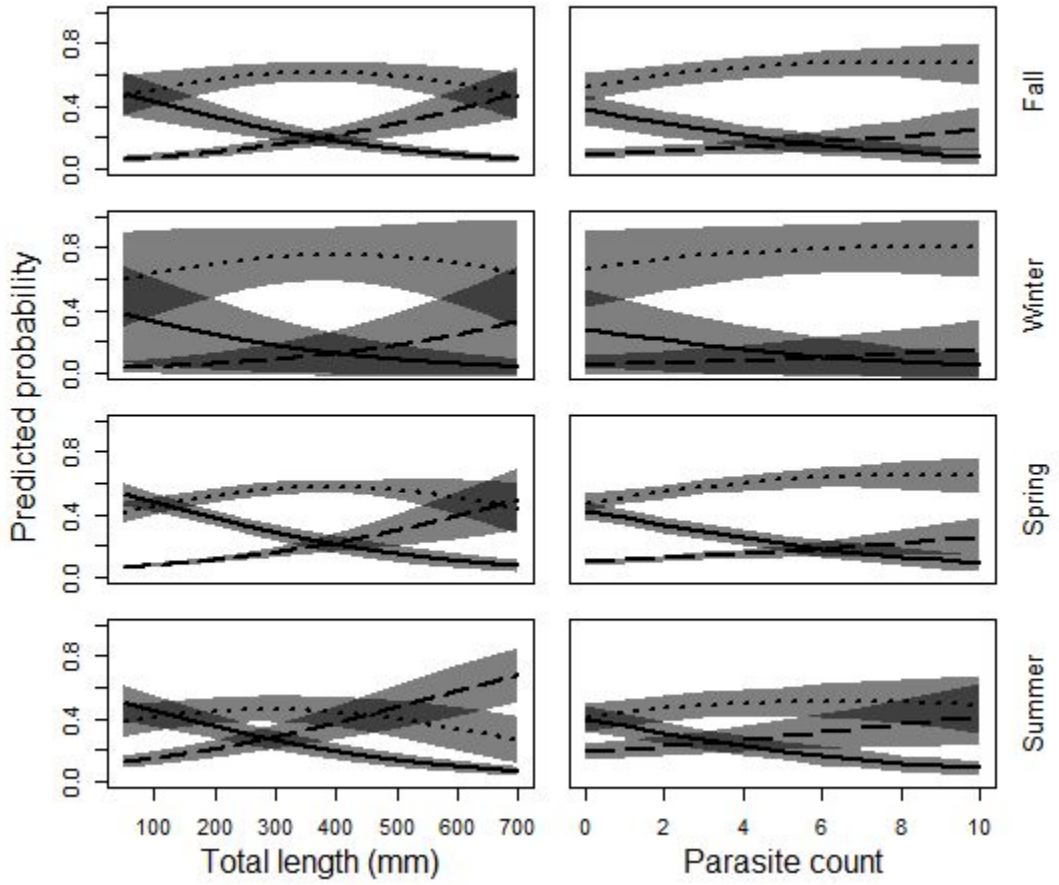

Figure 4. Predicted probability of elver and yellow eels being in a swimbladder condition category (low = SDI 0-1, ——— ; moderate = SDI 2-3, ····· ; severe = SDI 4-6, – – –) by season of capture, total length (left panel), and *A. crassus* parasite count (right panel). Total length is held constant at its mean in right panel and parasite count is held constant at its mean in the left panel. Results are from the ordinal logistic regression with catch ID as a random effect.

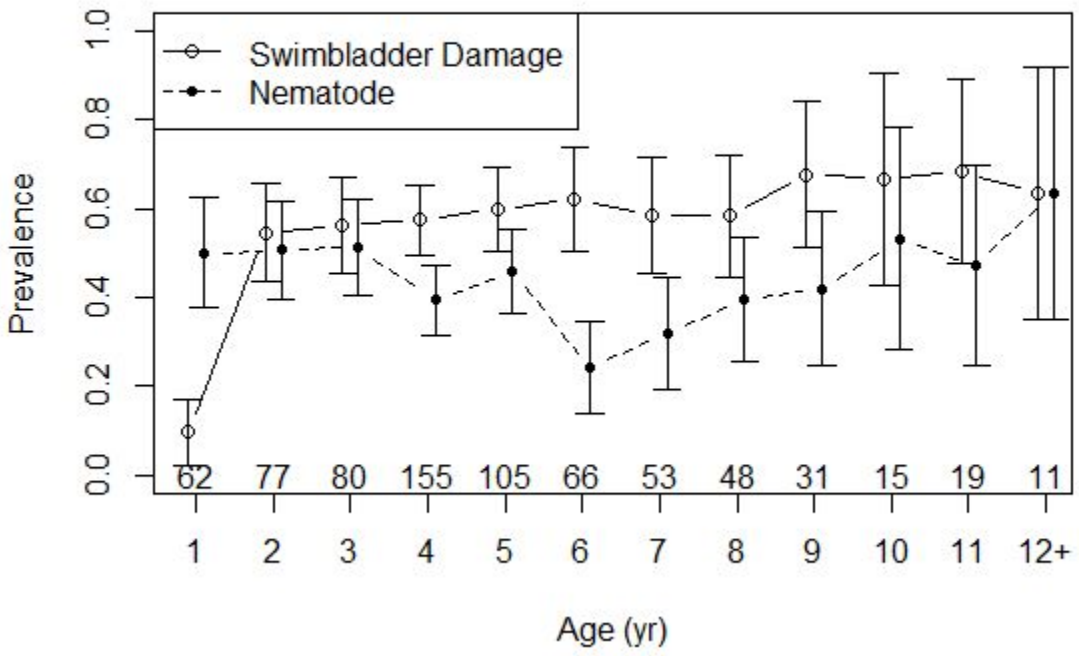

Figure 5. Prevalence of swimbladder damage (SDI≥3; open circles with solid line) and *A. crassus* (closed circle with dashed line) prevalence by age of elver and yellow American eels with confidence intervals. Numbers above x-axis indicate sample size in each age group. Points are slightly offset for clarity.

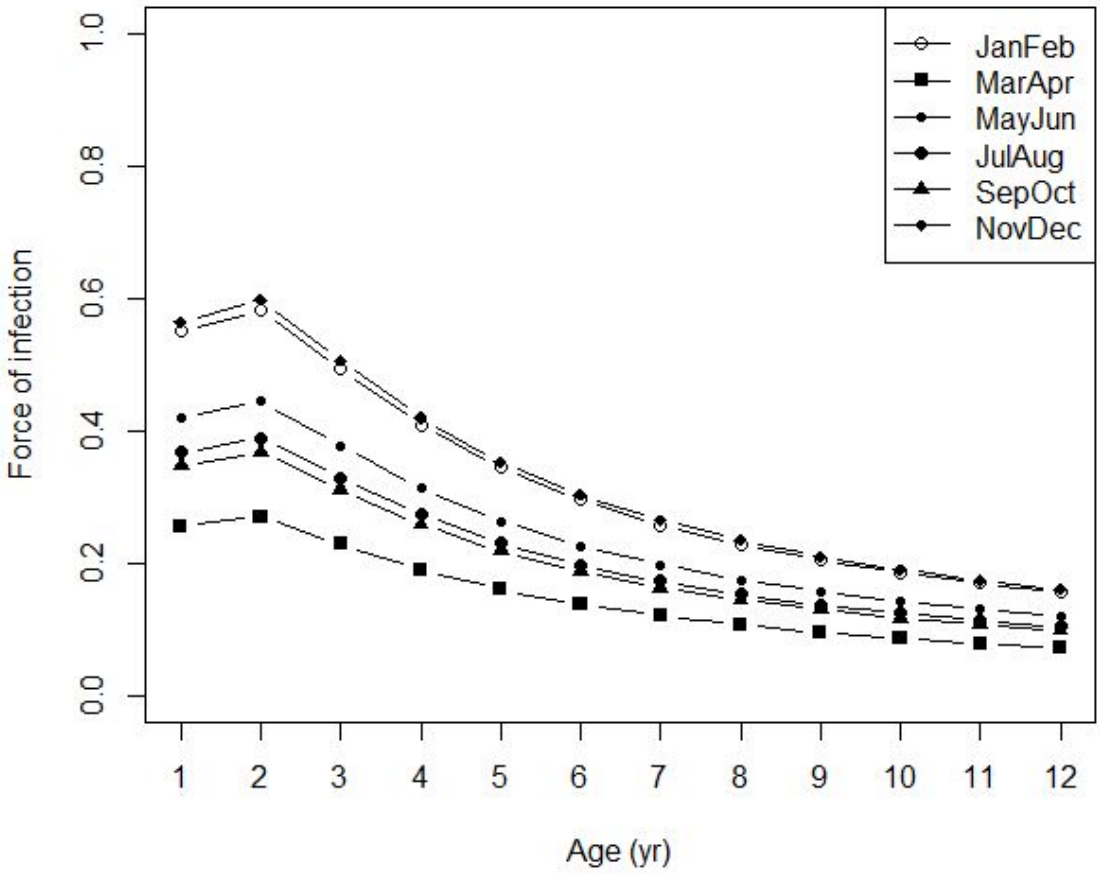

967

968 Figure 6. Force-of-infection of swimbladder damage by age for elver and yellow American eels
969 by month pairs from best fitting force-of-infection model (log-logistic, month pair, mortality).

970

971
972
973
974
975
976
977
978
979
980
981
982
983